STRUCTURED HIERARCHICAL MODELS FOR PROBABILISTIC INFERENCE FROM PERTURBATION SCREENING DATA

BY SIMON DIRMEIER[a] AND NIKO BEERENWINKEL[b]

Department of Biosystems Science and Engineering, ETH Zurich, [a]*simon.dirmeier@bsse.ethz.ch,*
[b]*niko.beerenwinkel@bsse.ethz.ch*

Genetic perturbation screening is an experimental method in biology to study cause and effect relationships between different biological entities. However, knocking out or knocking down genes is a highly error-prone process that complicates estimation of the effect sizes of the interventions. Here, we introduce a family of generative models, called the *structured hierarchical model* (SHM) for probabilistic inference of causal effects from perturbation screens. SHMs utilize classical hierarchical models to represent heterogeneous data and combine them with categorical Markov random fields to encode biological prior information over functionally related biological entities. The random field induces a clustering of functionally related genes which informs inference of parameters in the hierarchical model. The SHM is designed for extremely noisy data sets for which the true data generating process is difficult to model due to lack of domain knowledge or high stochasticity of the interventions. We apply the SHM to a pan-cancer genetic perturbation screen in order to identify genes that restrict the growth of an entire group of cancer cell lines and show that incorporating prior knowledge in the form of a graph improves inference of parameters.

1. Introduction. Probabilistic graphical models (PGMs) and Bayesian hierarchical models (HMs) are integral parts of statistical data analysis and computational biology. PGMs graphically represent the joint probability distribution of several random variables by encoding conditional dependencies between variables as edges in a graph (Koller and Friedman (2009), Maathuis et al. (2018)). Bayesian HMs are a special case of PGMs, where the graph is usually a directed tree and parameters of interest are endowed with distributions which themselves are parametrized leading to a conditionally independent hierarchy of variables (Gelman et al. (2013)).

In bioinformatics and computational biology, PGMs have been found to be especially useful and have a long history of applications, because biological measurements, such as gene expression values or metabolite concentrations, are often correlated making them suitable for joint probabilistic modelling. Simple PGMs, such as hidden Markov models (Durbin et al. (1998), Baldi et al. (1994), Eddy (1998), Stanke and Waack (2003), Marioni, Thorne and Tavaré (2006), Yoon (2009), Finn, Clements and Eddy (2011)) have been discussed in the bioinformatics literature at length.

Bayesian networks (BNs), a more general class of graphical models, where the underlying graph is a directed acyclic graph (DAG), are computationally more expensive, but probabilistically more expressive. For instance, Kuipers et al. (2018) used BNs to identifiy gene-gene interactions in cancer tissues and for clustering the mutational profiles of cancer types. Other approaches include Jansen et al. (2003) who used BNs to detect protein-protein interactions (PPIs) from genomic data, such as gene expression values, that is, the abundance of messenger RNA (mRNA) of a gene in the cell, Friedman et al. (2000) where BNs were applied to

model gene interactions and analyze expression data, or Sachs et al. (2005) who used BNs to reconstruct signalling networks. For time-series data, dynamic Bayesian networks (DBNs) have been used to, for instance, to identify gene regulatory networks (Murphy, Mian et al. (1999), Zou and Conzen (2004), Li et al. (2011), de Luis Balaguer and Sozzani (2017)).

In contrast to BNs, Markov random fields (MRFs) use undirected edges to encode conditional dependencies. Wei and Li (2007) and Chen, Cho and Zhao (2011) used MRFs to encode biological pathways and successfully identified single genes related to diseases. Krumsiek et al. (2011) used Gaussian MRFs to model the partial correlations among metabolites and showed that strong correlations often correspond to pathway interactions. Furthermore, in a recent study Schubert et al. (2019) used binary MRFs (Ising models) to model genetic interactions in order to predict epistatic loci that affect antibiotic resistance. For analysis of time-series gene expression data, Wei and Li (2008) used a spatio-temporal MRF that models the time- course of the differential gene expression stages. Recent approaches involving graphical models and network inference in biological applications have, for instance, been reviewed in Hawe, Theis and Heinig (2019).

HMs have gained widespread attention in modelling of biological data, on the one hand, due to their ability to represent and model the structure of many data sets, for instance, the nested structure of data, when, for multiple genes, measurements have been made in multiple conditions (e.g., tissues, cancer types, viruses, patients), and on the other hand, because biology itself is inherently hierarchical, for instance, between genes, transcripts, and proteins. Approaches utilizing hierarchical models are, for instance, presented in Fusi et al. (2014), Rakitsch et al. (2012), Zhou and Stephens (2012), Korte et al. (2012), Loh et al. (2015).

HMs can share statistical strength for parameter estimation across hierarchy levels. If we can infer parameters well in one group of the hierarchy, it can help to infer parameters well in another. In addition, for Bayesian HMs the choice of appropriate priors can induce an auto-regularizing effect, which makes HMs suitable for low sample size scenarios. A drawback of HMs is that one cannot assess statistical significance of the random effect estimates themselves, even in the frequentist setting

HMs have been found especially useful for the analysis of biological interventional data, such as genetic perturbation screens. In these screens, the variables of interest are artificially intervened on by an experimental perturbation. The intervention can either be conducted on a genomic level through loss-of-function mutations (knock-out), or the transcriptomic level by post-transcriptional gene silencing (knock-down), or post-translationally on the proteomic level. On the genomic level, the CRISPR-Cas9 system (Jinek et al. (2012), Doudna and Charpentier (2014)), where small guide RNAs (gRNAs) are used to direct a Cas9 protein to a target gene and a missense mutation is induced, has become the method of choice. One of the most frequent applications of genetic perturbation screening is measurement of downstream causal effects after the intervention. These effects can, for instance, be changes in transcript expression of certain genes when the perturbed gene was a transcription factor, or alteration of the viability of a pathogen (Rämö et al. (2014), Dirmeier et al. (2020)) or of a cancer cell line (Cowley et al. (2014), Aguirre et al. (2016), Meyers et al. (2017), Patel et al. (2017)). Viability is usually defined and measured as the log-fold change of the number of surviving cells pre- and post-intervention. The main interest in viability screens is to find genes that upon loss-of-function induce restricted or enhanced proliferation of cells or pathogens. Therapeutically, genes that enhance the growth of cancer cell lines or pathogens are of particular interest, since these genes can serve as potential drug targets for disease treatment. Estimation of the overall effect of a genetic perturbation, or more generally of a perturbation of a gene within a specific tissue or condition, is therefore of critical importance to learn more about disease biology and which genetic factors are involved in disease progression.

However, genetic perturbation screens are often accompanied by several persisting problems. While improvements in the design and analysis of experiments, such as the composition

of nucleotides of gRNA sequences (Doench et al. (2014), Xu et al. (2015)) or using appropriate noise models (Imkeller et al. (2019)), have been made, genetic perturbation screens still suffer from elevated false negative and false positive rates and bias of estimated effect sizes of the knock-outs (Munoz et al. (2016), Ong et al. (2017), Zhu et al. (2019), Meyers et al. (2017)). This is due to the fact that, while the biochemical process of an intervention is well understood, other factors, such as off-target effects, gRNA cytotoxicity, and binding affinity, can severely impact the success of an intervention (Wu et al. (2014), Doench et al. (2016)). For instance, off-target effects might lead to perturbation of a gene which is nonessential, rather than the targeted gene which induces cell death. Similarly, high cytotoxicity of a gRNA might induce cell death, while an intervention in the target gene itself is neutral. Other sources of error include stochasticity of transport of a gRNA into a cell, copy number alterations in cancer, multiplicity of infection, and low sequencing depth. Hence, not only is our understanding of complex biological systems and the interactions of their entities still limited, but also our understanding of the process responsible for generating the data. Due to imperfect interventions, readouts of perturbations screens are often noisy and confounded and a good model considering all relevant covariables is challenging to determine.

In addition, biological screening historically faces another problem, namely low sample sizes due to high costs of genome-wide experimentation. Public genome-wide perturbation data, such as provided in the DepMap portal (Tsherniak et al. (2017)), often only have as little as four replicates or less per intervention. Assessing causal effects and estimation of parameters is therefore difficult. In these settings, HMs are useful due to auto-regularization and borrowing of statistical strength, even though other approaches such as regularized linear models (Schmich et al. (2015)) or empirical Bayesian procedures exist (Love, Huber and Anders (2014), Robinson, McCarthy and Smyth (2010), Li et al. (2014)).

A promising extension of graphical and hierarchical modelling would be to combine the two approaches. PGMs are useful for probabilistically modelling biological prior information, for example, in the form of networks, which can then be used for the analysis of data sets using HMs. While the idea of incorporating networks for biological data analyses is not new, (Dirmeier et al. (2017), Li and Li (2008), Chen et al. (2012), Kim and Xing (2012), Zitnik, Agrawal and Leskovec (2018), Zamora-Resendiz and Crivelli (2019)), combining PGMs with HMs to aid and inform inference of posterior distributions has to our knowledge received only little attention.

Here, we propose *structured hierarchical models* (SHMs), a family of models that allows incorporating biological prior knowledge in the form of graphs directly into probabilistic analyses. The main idea is to use a categorical MRF as latent labelling, that is, clustering of genes, in order to probabilistically encode the pairwise relationships of genes using biological networks (Figure 1). Genes that are functionally related and are neighbors in the graph
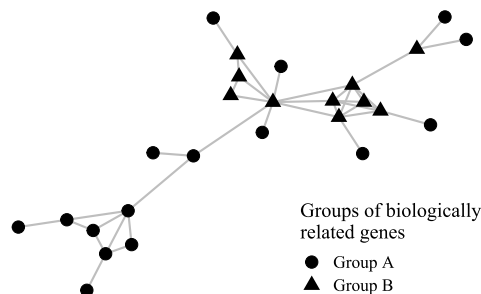

FIG. 1. *A biological network of gene-gene interactions that consists of two groups of genes, A and B. Edges define functional relationships between two genes. We use a Markov random field to encode similarities of pairs of genes, where neighboring genes have a higher probability to be in the same group than in a different one.*

have a higher probability to belong to the same cluster than to a different one. For example, for cell-viability assays, the clustering would label genes as essential or nonessential. If a gene is labelled as nonessential then the probability of its neighbors to also be nonessential is increased and vice versa. SHMs use the clustering of genes to inform the inference of parameters in an HM for which the data generating process is extremely noisy, difficult to model, and often yields erroneous inferences of parameters due to misspecification. The MRF pushes information of gene relationships downwards to inform the inference of parameters. In comparison to other methods that cluster variables in the data space, our method clusters data in the latent space of the gene effects. By encoding interactions of genes through a MRF we incorporate structural information into the inference. Since the model is fully Bayesian, appropriate choice of priors can furthermore have an auto-regularizing effect making it especially useful for low sample size scenarios.

The rest of the paper is organized as follows: we first introduce the SHM and its basic structure, that is, the core graphical model. We then show some empirical properties of the SHM in a study using simulated data, before we apply it to a biological data set from the DepMap portal (Tsherniak et al. (2017)). The DepMap data consists of multiple different cancer cell lines for which genome-wide perturbation screens have been conducted in quadruplicate. It is a low sample size data set of multiple conditions that due to the nature of perturbations should exert high variance. Inference of essential genes in multiple conditions is of great medical interest, because it could allow divising drugs with broad-spectrum activity. We conclude the paper with some remarks about Bayesian modelling and the SHM in general.

2. Structured hierarchical models. Genetic perturbation screens often exhibit high noise levels and are difficult to model due to frequent incomplete domain knowledge, high stochasticity of interventions, and low sample sizes. If perturbations are conducted for multiple conditions, such as cancer cell lines, the data have a nested structure which suggests a hierarchical modelling approach. We combine the hierarchical model with a categorical Markov random field to incorporate biological prior information in the form of networks to the model. We first describe the two model components separately and then introduce the SHM.

Bayesian hierarchical model. SHMs use Bayesian HMs as the first component to model a data set y_{gcn} with genes $g \in \{1, \ldots, G\}$, conditions $c \in \{1, \ldots, C\}$, for example, cell types, patients or tissues, and observations $n \in \{1, \ldots, n_{gc}\}$. The hierarchical model for the data set y_{gcn} is defined follows:

$$\tau_\gamma^2, \tau_\beta^2 \sim S_0,$$
$$\mu \sim \mathcal{N}(0, 1),$$
(1)
$$\gamma_g \mid \mu, \tau_\gamma^2 \sim \mathcal{N}(\mu, \tau_\gamma^2),$$
$$\beta_{gc} \mid \gamma_g, \tau_\beta^2 \sim \mathcal{N}(\gamma_g, \tau_\beta^2),$$
$$y_{gc} \mid \beta_{gc} \sim \mathbb{P}(h(\beta_{gc})).$$

The top level of the hierarchy consists of gene effects γ_g which describe the impact of a perturbation of a gene on the cell. The gene effects γ_g are modelled as normal random variable, with mean μ and standard deviation τ_γ. The level below consists of gene effects per condition β_{gc} which are parameterized by the gene effects γ_g and a standard deviation τ_β, and describe the effect of a perturbation on gene within a specific condition. We choose a unspecific joint prior distribution S_0 over $\tau_\gamma^2, \tau_\beta^2$ that can be specified appropriately, for

example, subjectively or by formal rules (Kass and Wasserman (1996), Gelman (2006), Kass and Natarajan (2006)). In the model definition above, we assume homoscedasticity of the errors τ_γ^2 and τ_β^2, but this is not a requirement and the distributions can be adapted, too. On the lowest level the random variables β_{gc} are used to model the distribution of the data which we assume to follow and exponential family distribution $\mathbb{P}$. For instance, for continuous data y_{gcn} might be normally distributed, while it could follow a Bernoulli distribution in the binary case. Like in a generalized linear regression model (GLM), we use a link function, h^{-1}, to relate the latent variable β_{gc} to the mean of the data.

Markov random field. The second component of an SHM is a categorical MRF $\mathbf{z} \in \{1, \ldots, K\}^G$ that encodes the assignment of a gene g to one of K components, for example, clusters of essential and nonessential genes. The categorical variables $\mathbf{z}$ are distributed

$$(2) \qquad \mathbf{z} \sim \frac{1}{Q} \exp\left(\zeta \sum_{(i,j) \in \mathcal{E}} \phi_{ij}(z_i, z_j) \right),$$

where Q is a normalization constant, ζ is a weight, and $\mathcal{E}$ are the edges of a biological network, such as a PPI. The functions ϕ_{ij} are potentials defined as

$$(3) \qquad \phi_{ij}(z_i, z_j) = \mathrm{diag}(w_{ij}, \ldots, w_{ij}).$$

The hyperparameters w_{ij} are nonnegative edge weights of the network. Thus we encode biological prior knowledge of related genes as probability distributions where two genes i and j, if biologically related, have an increased probability of having the same label z_i and z_j.

Structured hierachical model. SHMs combine Bayesian HMs and categorical MRFs, by replacing the distribution of γ_g in equation (1) with a distribution conditioned on the MRF. The entire model is defined as follows (Figure 2):

$$\mathbf{z} \sim \text{Categorical-MRF}(\zeta),$$

$$\tau_{\gamma 1}^2, \ldots, \tau_{\gamma K}^2, \tau_\beta^2 \sim S_0,$$

$$\mu_1, \ldots, \mu_K \sim \mathcal{N}_K(0, 1),$$

(4)

$$\gamma_g \mid z_g, \boldsymbol{\mu}, \boldsymbol{\tau}_\gamma^2 \sim \mathcal{N}(\mu_{z_g}, \tau_{\gamma_{z_g}}^2),$$

$$\beta_{gc} \mid \gamma_g, \tau_\beta^2 \sim \mathcal{N}(\gamma_g, \tau_\beta^2),$$

$$y_{gc} \mid \beta_{gc} \sim \mathbb{P}(h(\beta_{gc})).$$

The top level of the hierarchy is now the categorical MRF from equation (2) (abbreviated for notational simplicity). We replace the univariate distributions of μ and τ_γ^2 in equation (1) with K-dimensional distributions. The MRF induces a clustering in the latent space of $\boldsymbol{\gamma}$ and not in the data space $\mathbf{y}$. We are primarily interested in grouping genes, that is, the variables $\boldsymbol{\gamma}$ and not the actual data, that is, the effect sizes of the replicates of single interventions y_{gcn}. In addition, clustering in the data space is not only too difficult due to the noisy readouts of biological interventions, but also hardly ever of biological interest. The rest of the model stays as in (1).

The SHM compensates misspecification or incomplete domain knowledge by pushing down biological prior knowledge using the top-level MRF through the different hierarchies, thereby informing inference of latent parameters γ_g and β_{gc}. More specifically, either the real data generating process of the biological system under study is unknown and not all covariables and confounders that take influence are measured or known, or we cannot include them
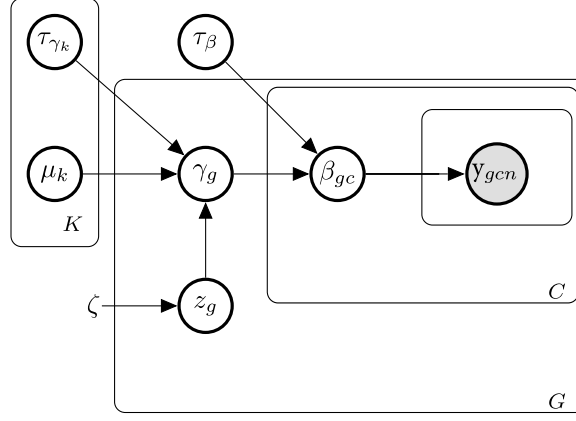
FIG. 2. *The basic structure of an SHM is a combination of a HM and a MRF. On the first level of the hierarchy of the HM we model the data y_{gcn} for a gene g, condition c and observation n as an exponential family distribution that is parameterized by a gene-condition effect β_{gc}. The gene-condition effect is modelled as a random variable with parameters γ_g, the gene effect, and a nuisance parameter τ_β. The gene effects are parameterized by a MRF z_g which clusters the latent gene effects, and vectors of means μ_{γ_k} and standard deviations τ_{γ_k}.*

as covariables, as inclusion would lead to ill-defined models that are not, or only weakly, identifiable, for example, in low sample size settings.

The model in equation (4) serves as a basic structure and needs to be adjusted for specific domains, that is, complemented with other covariables and appropriate distributions for the data at hand.

3. Models for genetic perturbation data. We use the backbone of the SHM (4) to build a concrete model for data from genetic perturbation screens. This requires specifying appropriate prior distributions for variance components and a distribution for the data, as well as supplementing the data generating process with appropriate covariables. For multi-condition genetic perturbation data sets we define the model as follows:

$$\mathbf{z} \sim \text{Categorical-MRF}(\zeta),$$

$$\tau_{\gamma_0}^2, \tau_{\gamma_1}^2 \sim \text{Inverse-Gamma}(5, 1),$$

$$\mu_0, \mu_1 \sim \mathcal{N}(0, 1) \quad \text{s.t. } \mu_0 < \mu_1,$$

$$\gamma_g \mid z_g, \boldsymbol{\mu}, \boldsymbol{\tau}_\gamma^2 \sim \mathcal{N}(\mu_{z_g}, \tau_{\gamma_{z_g}}^2),$$

$$\tau_\beta^2 \sim \text{Inverse-Gamma}(3, 1),$$

(5)
$$\beta_{gc} \mid \gamma_g, \tau_\beta^2 \sim \mathcal{N}(\gamma_g, \tau_\beta^2),$$

$$\tau_\iota^2 \sim \text{Inverse-Gamma}(3, 1),$$

$$\iota_i \mid \tau_\iota^2 \sim \mathcal{N}(0, \tau_\iota^2),$$

$$\sigma^2 \sim \text{Inverse-Gamma}(2, 1),$$

$$y_{gci} \mid \beta_{gc}, \iota_i, \sigma^2 \sim \mathcal{N}(\beta_{gc} + \iota_i, \sigma^2),$$

where we included variable ι_i to correct for effects an intervention might have, for example, cytotoxicity of the gRNA used for perturbation (note that this introduces another level of hierarchy for the interventions i). We choose inverse-Gamma distributions as priors for variance

components, following Kass and Natarajan (2006). The rest of the model is the same as in equation (4).

Following Meyers et al. (2017), if information of copy number aberrations c_{gc} is available, we include it as covariate for every gene and condition. Adjusting for copy number aberrations is necessary, because in regions of high copy number gain interventions can occur multiple times leading to a DNA damage response and cell cycle arrest. This in turn leads to no proliferation and observed readouts are low independent of the gene that has been perturbed. This part of the model then becomes

$$\beta_0 \sim \mathcal{N}(0, 1),$$

(6)

$$y_{gci} \mid \beta_0, \beta_{gc}, \iota_i, \sigma^2 \sim \mathcal{N}(c_{gc}\beta_0 + \beta_{gc} + \iota_i, \sigma^2),$$

where the parameters that are not endowed with priors are distributed as in model (5).

4. Model criticism. We evaluate our model using several simulated data sets and a biological data set from the DepMap portal to show that the inference of parameters can indeed be improved using biological prior knowledge. We compare SHMs to models, where we replace the MRF on top of the hierarchy of equation (4) with a conventional mixture model leaving the rest of the model identical. In this way we can assess the influence of the network itself.

We investigate the SHMs described in equations (5) and (6), and are interested in estimating effect sizes γ_g and classifying genes as essential ($z_g = 1$) or nonessential ($z_g = 0$), since these are the parameters of greatest biological importance. Thus we use $K = 2$ mixture components. Every gene g is perturbed using multiple different gRNAs i in multiple conditions c. If a gene is essential, i.e, $z_g = 1$, and has a negative gene effect, $\gamma_g < 0$, we expect to observe cell death upon intervention, while we expect no change in cell proliferation when the gene is nonessential and has an effect size $\gamma_g \approx 0$.

We first introduce criteria to evaluate the models, and then apply different SHMs to the data sets.

4.1. *Criteria of model criticism.* To evaluate the model, we are primarily interested in the estimates of the latent variables $\boldsymbol{\gamma}$ and $\mathbf{z}$. We assess the accuracy of the inference of the posterior of gene effects by comparing their estimated posterior means $\hat{\gamma}_g(\mathbf{y})$ to their true values γ_g using squared error loss

$$L(\hat{\gamma}_g, \gamma_g) = (\hat{\gamma}_g(\mathbf{y}) - \gamma_g)^2.$$

In order to assess the correct inference of posterior labels, we compare means of posterior labels $\hat{z}_g(\mathbf{y})$ to their true values z_g using the number of correct and incorrect classifications. Specifically, we estimate the number of true positives, that is, the number of predictions of correctly classifying a gene as

$$\#\text{TP} = \sum_g^G \mathbb{I}(\hat{z}_g(\mathbf{y}) \geq 0.5 \wedge z_g = 1)$$

and the number of false negatives as

$$\#\text{FN} = \sum_g^G \mathbb{I}(z_g = 1) - \#\text{TP}.$$

We evaluate the number of false positive inferences as

$$\#\text{FP} = \sum_g^G \mathbb{I}(\hat{z}_g(\mathbf{y}) \geq 0.5 \wedge z_g = 0)$$

and the number of true negatives analogously as

$$\#\text{TN} = \sum_{g}^{G} \mathbb{I}(z_g = 0) - \#\text{FP}.$$

We follow the hypothetico-deductive model of (Gelman and Shalizi (2013), Gelman et al. (2013)) to evaluate posterior inference visually by computing posterior predictive distributions (PPCs) and plotting them as density estimates over the data (Gabry et al. (2019)). The predictive posterior is computed as

$$(7) \qquad P(\tilde{\mathbf{y}} \mid \mathbf{y}) = \int P(\tilde{\mathbf{y}} \mid \boldsymbol{\theta}) P(\boldsymbol{\theta} \mid \mathbf{y}) \, d\boldsymbol{\theta},$$

where $\boldsymbol{\theta} = (\mathbf{z}, \boldsymbol{\gamma}, \dots)$ is a vector of all random variables of an SHM.

4.2. *Simulated data.* We first evaluate our model on multiple simulated data sets in order to show that including graph prior knowledge can indeed inform posterior inference when the data generation process is misspecified. Specifically, we compare the SHM in (5) to a model that uses the same hierarchical structure, but replaces the MRF (2) with a conventional mixture model, that is, we only replace the first line in (5) with

$$(8) \qquad \begin{aligned} \mathbf{p} &\sim \text{Dirichlet}(1, 1), \\ z_g &\sim \text{Categorical}(\mathbf{p}). \end{aligned}$$

Since the HM part is the same in both models, any differences in the inference of posteriors can only be explained through the MRF, or mixture model, respectively. We briefly describe the different steps how we generated the data sets for the validations:

1. Generate a scale-free network of genes using the `powerlaw_cluster_graph` function from `networkx` package (Hagberg, Schult and Swart (2008)).

2. Separate the genes of the networks into two groups, a group of essential genes and a group of nonessential genes.

3. For essential genes sample $\gamma_g \sim \mathcal{N}(-1, 0.25)$, for nonessential genes sample $\gamma_g \sim \mathcal{N}(0, 0.1)$ (argueing that genes with no effect should have a lower variance, since no effect should be measured).

4. Sample $\beta_{gc} \sim \mathcal{N}(0, 0.25)$.

5. Sample $\iota_i \sim \mathcal{N}(0, 0.1)$.

6. In order to simulate low-quality interventions i, set gRNA activity of some of the essential genes to $a_i = 0.1$ (we call these genes in the following essential genes with low affinity gRNA). For the other gRNAs we assume high-quality interventions setting $a_i = 1$.

7. Sample $y_{gci} \sim \mathcal{N}(a_i \beta_{gc} + \iota_i, \sigma^2)$ with $n = 10$ replicates for every combination of g, c and i and noise variances $\sigma^2 \in \{0.1, 0.2, 0.3, 1\}$.

Hence, in order to simulate misspecification, that is, in this case incomplete domain knowledge, we use a data generating process that includes a covariate for low-quality interventions a_i, but then model the simulated data without it. Incomplete domain knowledge is frequent in biology.

For the first validation, we were interested in the effect of low-activity gRNAs of essential genes when neighborhoods consist entirely of other essential genes (Figure 3(a)). For perfect interventions, that is, when all affinities $a_i = 1$ and the data generating processes are perfectly captured by models (5) and (8), the two models are identical, as no information of the labels of neighbors is needed, and hence inference should be the same (Figure 3(b), top). The posterior distributions of the gene effects γ_g and class assignments z_g of these genes illustrate this
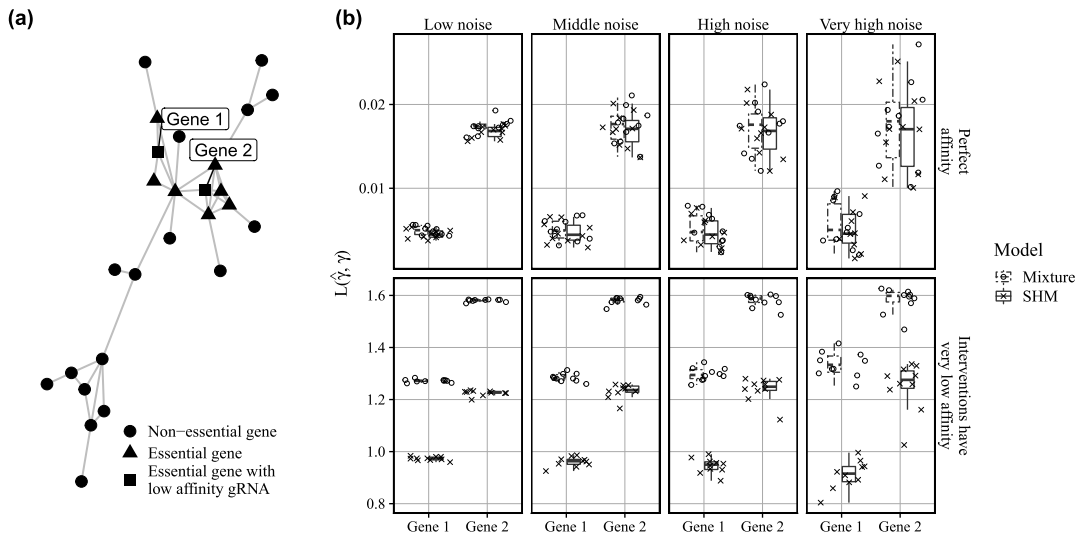
FIG. 3. *Benchmarking of parameter inference for genes that are embedded in neighborhoods of genes with the same label. (a) The network shows groups of essential genes (triangles/squares) and nonessential genes (circles). For essential genes depicted as squares we simulated data where some gRNAs have low activity, that is, where interventions do not work as intended and where the data does not show that the genes are essential. (b) Performance of the mixture model and the SHM. Every box shows the results of 10 simulated data sets and different noise levels. The y-axis shows the squared error loss of posterior means of gene effects of gene 1 and 2 (lower is better). If data are generated with perfect activity for the square nodes, the mixture and the SHM perform equally good as expected (top row). If we generate gRNAs with low activity for the two square nodes the SHM clearly outperforms the conventional mixture model (bottom row).*
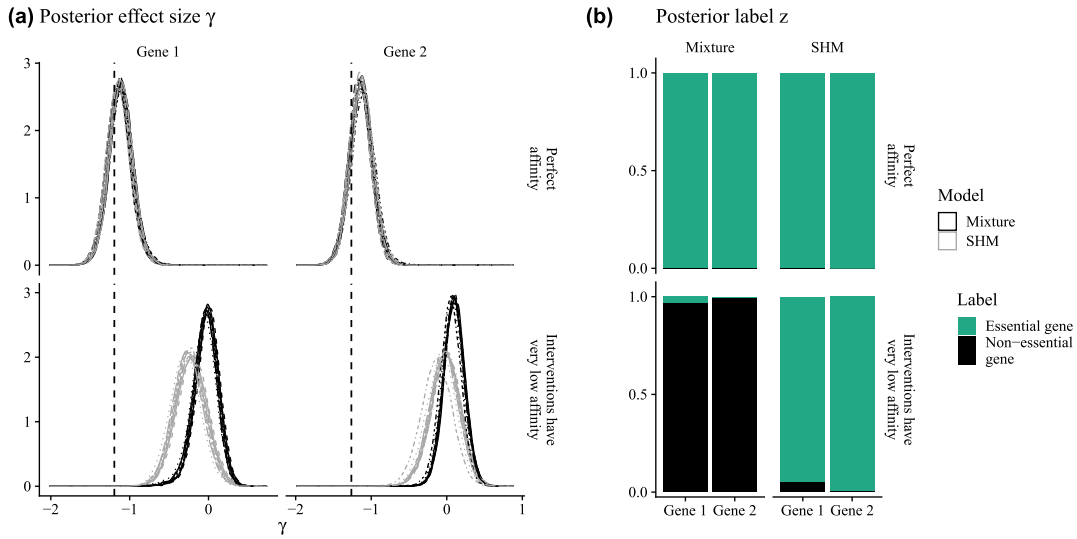

FIG. 4. *Posterior distributions of the effect sizes γ_g and labels z_g for genes that are embedded in neighborhoods of genes with the same label. The experimental setting is as in Figure 3, that is, the groups of the graph are the same and the squared nodes have low-activity gRNAs. (a) As expected the SHM and the mixture model infer the same posterior distributions when all interventions work as intended (top row). When some of the gRNAs have low activity, the SHM moves the posterior distribution closer to the true value (dashed line) and outperforms the mixture model (bottom row). (b) Both models infer the posterior probabilities of the labels z_g correctly when gRNAs work as intended (top row). In the case of low-affinity gRNAs, the SHM is still able to infer the correct labels, while the mixture model fails to do so (bottom row).*
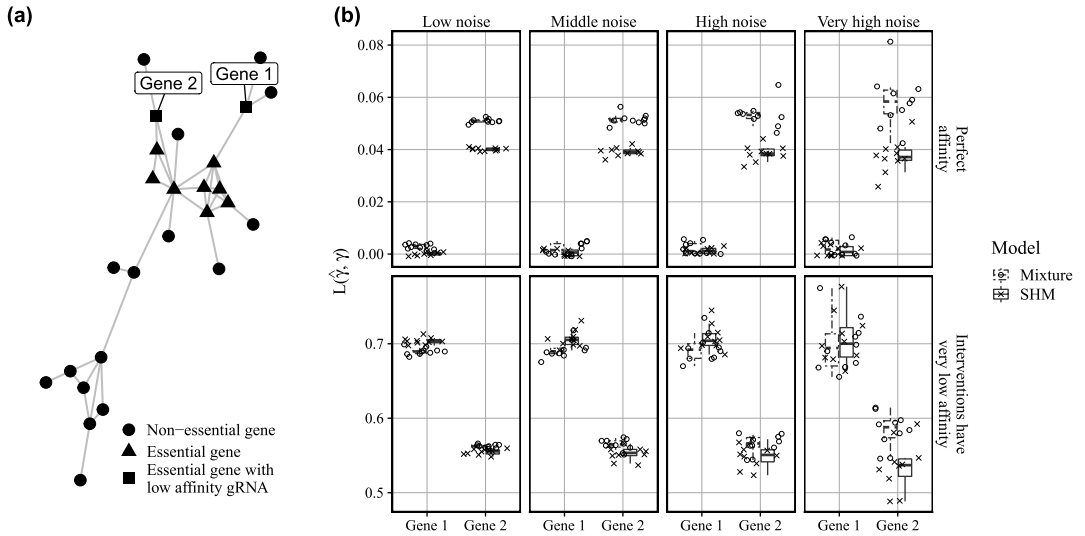
FIG. 5. *Benchmarking of parameter inference when the number of neighbors with the same label is one higher, or lower, than nonessential neighbors. (a) The network shows the same graph of genes as in Figure 3 with the difference that now genes depicted as squares belong to a different neighborhood. (b) When the number of essential and nonessential neighbors is roughly the same, the influence of the SHM vanishes and the data primarily informs inference. Hence, it is difficult to assume that the SHM outperforms the mixture model, even though the performances are improved for gene 2. For gene 1 the mixture model slightly outperforms the SHM. Generally, in scenarios where the number of essential and nonessential neighbors is the same, both models should perform similarly.*

(Figure 4, top). However, in the case of some gRNAs having low affinities the influence of the neighbors, mediated through the MRF, improves inference substantially (Figure 3(b), bottom; Figure 4, bottom).

We then assessed the influence of the MRF on inference when essential genes with low-affinity gRNAs have essential as well as nonessential neighbors (Figure 5(a)). In this case, as long as the essential genes with low affinities have more essential neighbors than nonessential ones, estimation of parameters improves. If there are more nonessential neighbors than essential ones, the mixture model has negligibly better performance than the SHM. Vice versa, if there are more essential neighbors, the SHM outperforms the mixture model. In general assessing settings where the number of essential and nonessential neighbors is roughly the same is difficult, because posterior inference will be dominated by the data itself and not the MRF, that is, the effect of the MRF vanishes, because the influence of essential and nonessential neighbors is equally strong and cancels out (Figure 5(b)). In these settings, both models achieve similar results.

Finally, we show how one can break our model, namely by embedding an essential gene with low-affinity gRNAs in a neighborhood of exclusively nonessential genes (Figure 6). The neighborhood then wrongly informs the inference of the gene's class assignment and the mixture model outperforms the SHM.

4.3. *Biological data.* We applied the SHM to a biological data set form the DepMap portal (Tsherniak et al. (2017), Meyers et al. (2017); data downloadable from Broad DepMap (2019)). The DepMap data consist of several cancer cell lines (conditions) for which genetic perturbation experiments using CRISPR have been conducted and the effects of a knockout on cell proliferation have been measured. If a gene is essential we expect to observe cell death upon intervention, while we expect no change in cell proliferation when the gene is not essential.
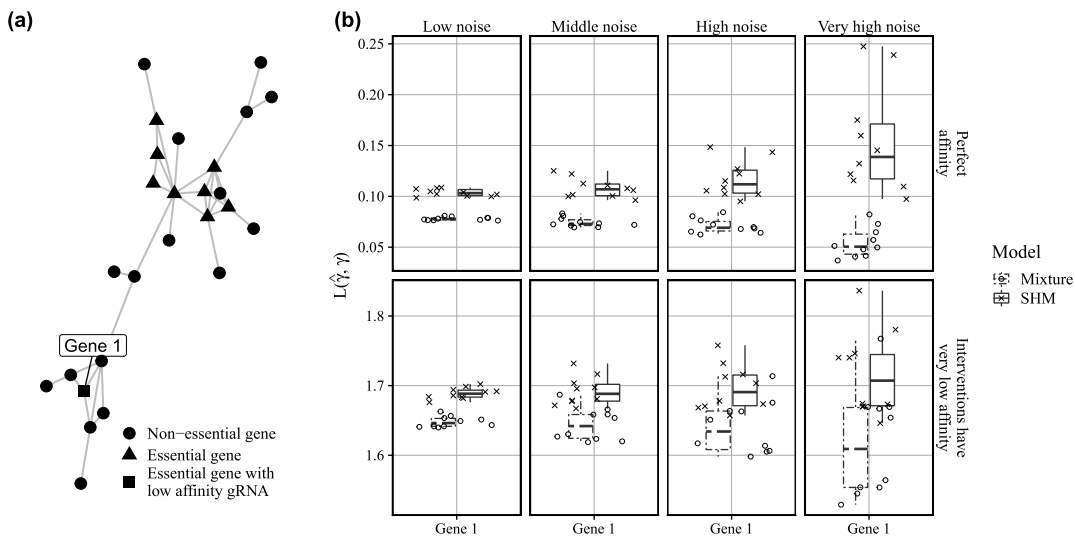
(a)

(b)

FIG. 6.   *Benchmarking of parameter inference for genes that are embedded in neighborhoods of genes with a different label.* (a) *The network shows the same graph of genes as in Figure 3 with the difference that now essential genes depicted as squares are surrounded by nonessential genes.* (b) *In this scenario the SHM wrongly informs posterior inference and the estimates of the effect sizes are worse in comparison to the mixture model, both for gRNAs with perfect affinity, as well as for gRNAs with lower affinity.*

We downloaded the data from the the DepMap portal and selected screens with $n = 4$ replicates and a sufficiently high Cas9 activity, leaving a total of 7 experiments (Table 1).

The DepMap data provides information about true essential and nonessential genes from (Hart et al. (2014), Hart et al. (2015)), that is, information on some of the genes regarding their label. In order to be able to validate our estimates, that is, whether we classified genes correctly, we reduced the set of genes to these controls, leaving roughly 500 genes. We used the SHM (6) to model the data.

The latent labels **z** are distributed as in equation (2) with edge potentials as defined in equation (3) and constant weights $w_{ij} = 1$. We downloaded the String PPI network (Szklarczyk et al. (2018)) and removed all edges with low confidence, that is, edges with a score of less than 500 (Figure 7). This step is done in an effort to reduce potential false positive edges, that is, edges erroneously inferred using yeast two-hybrid (Y2H) or other technologies to detect PPIs. In the network, essential genes and nonessential genes seem to be surprisingly well separated. Curious about this finding, we compared this network with the functional network from (Wu, Feng and Stein (2010)) and the physical interaction network from (Oughtred et al. (2018)) and found that both groups of genes were equally well separated in these networks,

TABLE 1
Meta data of the biological data set from the DepMap portal

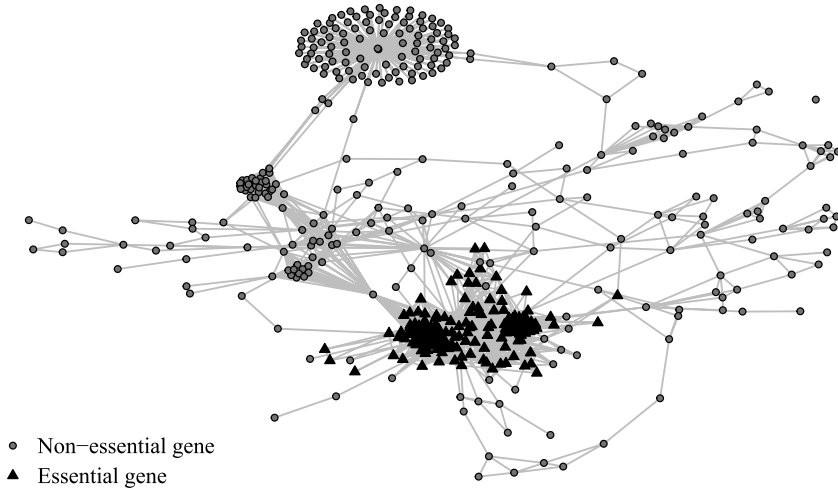| ID	Cell-line	Disease	Disease subtype	Set
ACH-000120	CHP212	peripheral nervous system	neuroblastoma	train
ACH-000414	NCIH1944	lung	lung NSC	train
ACH-000841	NCIH2087	lung	lung NSC	train
ACH-000312	SKNBE2	peripheral nervous system	neuroblastoma	test
ACH-000226	SUPM2	lymphoma	ALCL	test
ACH-000311	NCIH2122	lung	lung NSC	test
ACH-000118	HUPT3	pancreas		test

FIG. 7. *Biological network used for inference of essential genes from the DepMap data. In order to apply the SHM to real data, we downloaded the STRING network that encodes gene-gene interactions. For visualization we also downloaded information about gene essentiality and show the respective node label using different shapes. Essential genes seem to cluster into modules of high-connectivity* (*compare Supplementary Figure* 1 (*Dirmeier and Beerenwinkel* (2022))).

although not all genes from the DepMap data were contained in them, which possibly explains the high number of singletons in these networks (Supplementary Figure 1 (Dirmeier and Beerenwinkel (2022))).

Since the DepMap portal provides estimates of the activity of gRNAs (Doench–Root scores), that is, quantification how well a gRNA works, we fit a second model that has an additional covariate for gRNA affinity a_i, but is otherwise identical to (6). For most other experiments, estimates of gRNA affinity are not available and we were only able to include it here. The data generating process then changes to

$$(9) \qquad y_{gci} \mid \beta_0, \beta_{gc}, \iota_i, \sigma^2 \sim \mathcal{N}\big(a_i(c_{gc}\beta_0 + \beta_{gc}) + \iota_i, \sigma^2\big).$$

We first estimated the hyperparameter ζ using a grid search in $[0.05, 0.1, \ldots, 1]$ with training data consisting of three cell lines (train data sets in Table 1) resulting in an optimal estimate of $\zeta = 0.15$. We then inferred the parameters of the models using test data of four cell lines (Table 1). As in the simulated data benchmarks, we compared the model against a model where the MRF is replaced with a conventional mixture model (equation (8)) with two components. As before, with this approach differences in the parameter estimates are due to the MRF alone, and not the HM. We are assessing in total four different models (Table 2).

We found that in both cases biological prior information improved inference of the posterior labels (Figure 8). While the models with Doench–Root scores are very similar and the improvement of the SHM is only marginal, reducing the number of false negatives from 8 to

TABLE 2
Overview of different models used for model criticism with biological data

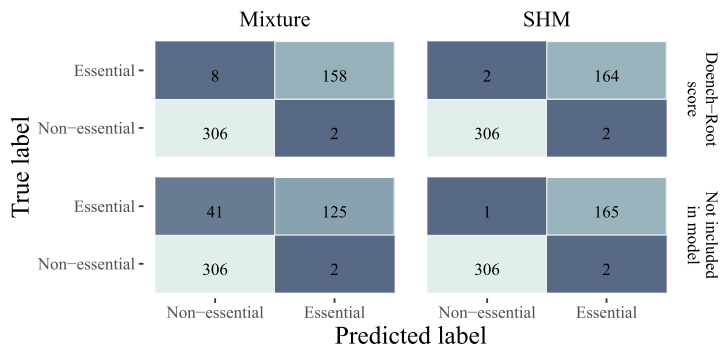| Prior	gRNA activity	Description
MRF	no	HM (6) + MRF (2)
Mixture	no	HM (6) + mixture model (8)
MRF	yes	HM (9) + MRF (2)
Mixture	yes	HM (9) + mixture model (8)

FIG. 8. *Confusion matrices of true and estimated essential genes of four biological models inferred from the DepMap data. Every confusion matrix shows the number of false positives and false negatives for each model (Table 2). The SHM outperforms the mixture models if Doench–Root scores, that is, covariables quantifying gRNA activity, are included by reducing the number of false negatives from 8 to 2 (top row). When Doench–Root scores are not included, the number of false negatives is reduced from 41 in the mixture to 1 in the SHM (bottom row).*

2, the improvement of the SHM over the clustering model when not including the Doench–Root score is substantial: we reduce the number of FNs from 41 to 1. Interestingly we do not observe improvement in false positives (all 2), which emphasizes our initial hypothesis: inference of essential genes is mainly a problem of high false-negative rates and not of false-positive rates. To further corroborate this hypothesis, we fit the simplest conceivable model to infer gene labels **z**. Specifically, we used a naive one-dimensional Gaussian mixture model directly on the average gene depletion scores computed over all tissues and sgRNAs. Applying this model resulted in 21 false negatives, but zero false positives (see Supplementary Figures 5 and 6 for more details (Dirmeier and Beerenwinkel (2022))). Between the SHM models there are hardly any improvements, underlining our hypothesis that better, more robust inferences form noisy data sets can be made when network information is incorporated. On the other hand, the results of the mixture models are very different which emphasizes
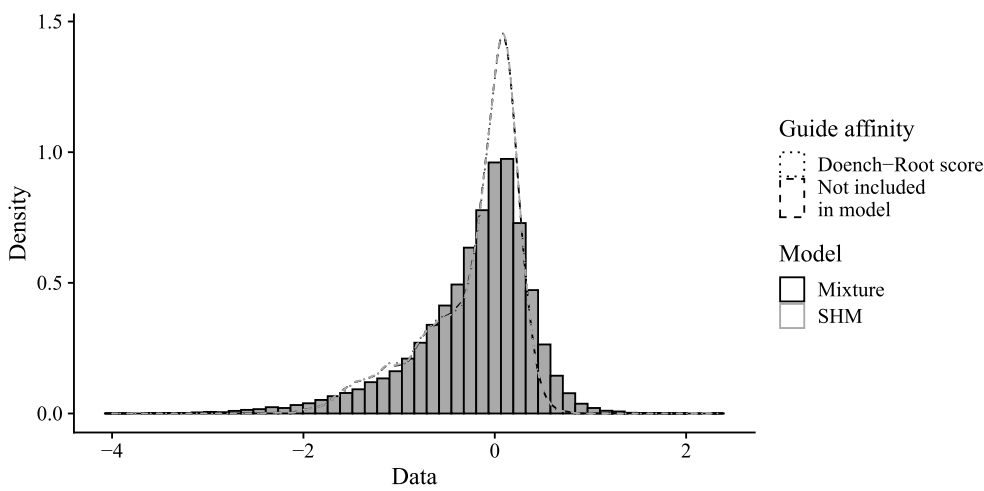

FIG. 9. *Posterior predictive distributions (PPCs) of the DepMap genetic screening data sampled using four biological models (Table 2). We sampled data from the posterior predictive distributions using equation (7) and overlayed the histogram of the original biological data set with the kernel denisty estimates of the sampled data. All four models can adequately predict new data from the posterior distributions. The density curves are close to the original data, especially in the lower tail of the histogram. The PPCs underestimates the upper tail of the histogram slightly.*

the fact that careful model building is required for interventional studies, a problem that gets aggravated with missing domain knowledge.

Considering the posterior predictive distributions of the four models that we fit, we found the distributions to be almost identical (Figure 9). This shows that the main differences are mainly in inferring the nested parameters, while the actual data generating process stays the same.

5. Implementation. The graphical model representation of the SHM in (2) has a tree structure (Figure 2) which allows for Gibbs sampling to infer posterior distributions. In particular, we developed a custom Metropolis-within-Gibbs sampler using the probabilistic programming language `PyMC3` (Salvatier, Wiecki and Fonnesbeck (2016)). Here, we show how one can simulate from the posterior distribution of the SHM in equation (4). The sampler can be easily extended to more complex models with more covariates and latent variables, as long as the Markov blanket of the class labels $\mathbf{z}$ stays the same.

We denote by D the data and $\boldsymbol{\theta} = (\boldsymbol{\beta}, \boldsymbol{\gamma}, \tau_\beta^2, \boldsymbol{\mu}, \boldsymbol{\tau}_\gamma^2, \sigma^2)$ the continuous parameters of the model. The full posterior of equation (4) has the following form:

$$
\begin{aligned}
(10) \qquad P(&\boldsymbol{\theta}, \mathbf{z} \mid D) \\
&\propto P(D \mid \boldsymbol{\beta}, \sigma^2) \cdot P(\boldsymbol{\beta} \mid \boldsymbol{\gamma}, \tau_\beta^2) \cdot P(\tau_\beta^2) \cdot P(\sigma^2) \\
&\quad \cdot P(\boldsymbol{\gamma} \mid \mathbf{z}, \boldsymbol{\mu}, \boldsymbol{\tau}_\gamma^2) \cdot P(\mathbf{z}) \cdot P(\boldsymbol{\mu}) \cdot P(\boldsymbol{\tau}_\gamma^2).
\end{aligned}
$$

For every iteration t, a sample $(\boldsymbol{\theta}, \mathbf{z})^t$ from the full posterior using Metropolis-within-Gibbs can be obtained in two steps:

1. draw $\mathbf{z}^t$ from $P(\mathbf{z} \mid D, \boldsymbol{\theta}^{t-1}) \propto P(\boldsymbol{\gamma} \mid \mathbf{z}, \boldsymbol{\mu}, \tau_g) \cdot P(\mathbf{z})$ using Gibbs sampling,
2. draw $\boldsymbol{\theta}^t$ from $P(\boldsymbol{\theta} \mid D, \mathbf{z}^t)$ using Hamiltonian Monte Carlo.

Developing the Metropolis-within-Gibbs sampler with `PyMC3` only requires implementing a custom sampler for the Markov random field $\mathbf{z}$ in step one (the Appendix for more details). For the continuous variables $\boldsymbol{\theta}$ we use a Hamiltonian Monte Carlo (HMC) (Neal (2011), Betancourt (2017)) variant, the No-U-Turn sampler (Hoffman and Gelman (2014)), provided by `PyMC3`. In order to avoid divergences and for efficiency, we use a noncentered parameterization whereever possible (Betancourt and Girolami (2015)).

We implemented the sampler described above in a Python package which is available from GitHub at github.com/cbg-ethz/shm. The GitHub repository also contains the implementations for the models used in Section 4.

6. Discussion. We introduced a new family of models, the *structured hierarchical model* (SHM), which combines Bayesian hierarchical models with categorical Markov random fields. Through the random field, it is possible to aid posterior inference by probabilistically incorporating biological network information into the model. Since the random field introduces a latent categorical variable $\mathbf{z}$ which is used to parameterize the hierarchical model, we induce a mixture model of the top-level latent variables of the hierarchical model. In our application of perturbation data, the clustering allowed labelling genes as essential or nonessential. However, the model is also applicable to more general labeling tasks which require separation of genes into different classes, such as, for example, identifying differentially expressed genes from RNA-seq data or host dependency and restriction factors from viral or bacterial perturbation screens.

We applied the SHM to simulated data as well as to a biological data set from the DepMap portal and found that including biological prior knowledge generally improves estimation of

parameters. The biological networks we considered were all very similar in grouping functionally related genes together in a biological meaningful way. In practice, the choice of networks depends on the task at hand. For instance, for inference of essential genes, the networks by Szklarczyk et al. (2018), Wu, Feng and Stein (2010), and Oughtred et al. (2018), that is, physical interaction and functional networks, were found to be suitable. Others, such as gene regulatory networks, which encode a different type of information likely less relevant for inference of essential genes, might incorrectly inform posterior inference. Hence, as all prior elicitation, the choice of the network that encodes the random field prior should be done with care and using domain expertise.

The SHM is especially useful for noisy data sets consisting of multiple conditions which are common in interventional, biological studies. We expect our model to be of use for computational biologists, because it demonstrates how to coherently incorporate biological networks into probabilistic analyses. For the inference of parameters, HMs borrow statistical strength from other hierarchy levels. Additionally, when choosing appropriate priors, Bayesian inference has an auto-regularizing effect which makes it applicable even for data sets with low sample size. Consequently, Bayesian HMs are very useful in different branches of computational biology, powerful tools due to their statistical properties, and easily interpretable.

However, the SHM also has some drawbacks. In general, full Bayesian inference using sampling is computationally highly demanding and can be difficult, for instance on a genome-wide scale. Sampling is further complicated due to the high-dimensional categorical variable $\mathbf{z}$, because sampling discrete parameters usually yields low effective sample sizes and thus requires long chains for convergence. While we usually marginalize out $\mathbf{z}$ in conventional mixture models, this cannot be done here due to the conditional dependencies encoded in the MRF.

Furthermore, not much research has focussed on the theoretical and practical properties of combining an HMC for continuous parameters with a Gibbs sampler for discrete ones. In order to speed up posterior inference, approaches using variational inference could be adopted, but would require to either continuously relax or reparameterize the discrete Markov random field $\mathbf{z}$, for example, as in Jang, Gu and Poole (2017) or Guo and Schuurmans (2006). Applying reparameterization to conditionally dependent random variables has not received much attention by researchers though. Thus, a natural, non-Bayesian approach could be *maximum a posteriori* (MAP) inference, or approximate approaches such as empirical Bayes (Efron (2012)). MAP inference, however, has the obvious drawback of not yielding uncertainty estimates.

The SHM described in equation (4) represents a basic structure which needs to be adjusted to specific domains. Hence, we did not specify priors for variance parameters. In our analyses above, the use of inverse-Gamma distributions for variance parameters has no real justification other than being weakly-informative and conditionally conjugate. While for the sake of demonstration of the SHM this is acceptable, in general, one can follow principled ways for prior specification, such as (Gelman (2006), Gelman, Simpson and Betancourt (2017), Kass and Wasserman (1996)). Consequently, the SHM serves rather as a framework for probabilistic programs which requires careful adaption to different domains, rather than compromising a fit-for-all model for general Bayesian inference in perturbation screens.

We hope our contributions will be only a first step towards integrating biological prior knowledge into probabilistic models and that more research is invested into the topic in general and into efficient (variational) approximations in particular.

APPENDIX: GIBBS SAMPLING A CATEGORICAL MRF

Denote D the data and $\boldsymbol{\theta} = (\boldsymbol{\beta}, \tau_\beta, \sigma^2)$ (note that we use different notation for $\boldsymbol{\theta}$ as before). The first step of the Metropolis-within-Gibbs sampler draws the posterior $P(\mathbf{z} \mid$

$D, \boldsymbol{\theta}, \boldsymbol{\gamma}, \boldsymbol{\mu}, \boldsymbol{\tau}_\gamma^2$). Following Wainwright and Jordan (2008), a sample is obtained by conditioning on the Markov blanket of $\mathbf{z}$, which is

$$
\begin{aligned}
P(\mathbf{z} \mid D, \boldsymbol{\theta}, \boldsymbol{\gamma}, \boldsymbol{\mu}, \boldsymbol{\tau}_\gamma^2) &= \frac{P(\mathbf{z}, D, \boldsymbol{\theta}, \boldsymbol{\gamma}, \boldsymbol{\mu}, \boldsymbol{\tau}_\gamma^2)}{P(D, \boldsymbol{\theta}, \boldsymbol{\gamma}, \boldsymbol{\mu}, \boldsymbol{\tau}_\gamma^2)} \\[2mm]
&= \frac{P(\mathbf{z}, D, \boldsymbol{\theta}, \boldsymbol{\gamma}, \boldsymbol{\mu}, \boldsymbol{\tau}_\gamma^2)}{\sum_{\mathbf{z}} P(\mathbf{z}, D, \boldsymbol{\theta}, \boldsymbol{\gamma}, \boldsymbol{\mu}, \boldsymbol{\tau}_\gamma^2)} \\[2mm]
&\overset{\text{Use (10)}}{=} \frac{P(\boldsymbol{\gamma} \mid \mathbf{z}, \boldsymbol{\mu}, \boldsymbol{\tau}_\gamma^2) \cdot P(\mathbf{z})}{\sum_{\mathbf{z}} P(\boldsymbol{\gamma} \mid \mathbf{z}, \boldsymbol{\mu}, \boldsymbol{\tau}_\gamma^2) \cdot P(\mathbf{z})} \\[2mm]
&= P(\mathbf{z} \mid \boldsymbol{\gamma}, \boldsymbol{\mu}, \boldsymbol{\tau}_\gamma^2).
\end{aligned}
$$

We sample from $P(\mathbf{z} \mid \boldsymbol{\gamma}, \boldsymbol{\mu}, \boldsymbol{\tau}_\gamma^2)$ componentwise for every $z_i \in \{1, \ldots, K\}$, $i \in \{1, \ldots, G\}$ using a Gibbs-sampler:

$$
\begin{aligned}
P(z_i = k \mid \mathbf{z}_{-i}, \boldsymbol{\gamma}, \boldsymbol{\mu}, \boldsymbol{\tau}_\gamma^2) &= \frac{\exp(\sum_{(i,j)\in\mathcal{E}} \phi_{i,j}(z_i = k, z_j)) P(\gamma_i \mid \mu_{z_i=k}, \tau^2_{\gamma_{z_i=k}})}{\sum_{\tilde{k}\in K}[\exp(\sum_{(i,j)\in\mathcal{E}} \phi_{i,j}(z_i = \tilde{k}, z_j)) P(\gamma_i \mid \mu_{z_i=\tilde{k}}, \tau^2_{\gamma_{z_i=\tilde{k}}})]} \\[2mm]
&= \frac{\exp(\eta_k) P(\gamma_i \mid \mu_{z_i=k}, \tau^2_{\gamma_{z_i=k}})}{\sum_{\tilde{k}\in K}[\exp(\eta_{\tilde{k}}) P(\gamma_i \mid \mu_{z_i=\tilde{k}}, \tau^2_{\gamma_{z_i=\tilde{k}}})]},
\end{aligned}
$$
(11)

where we introduced $\eta_k = \sum_{(i,j)\in\mathcal{E}} \phi_{i,j}(z_i = k, z_j)$ for brevity. In the binary case, equation (11) can be simplified to

$$
\begin{aligned}
P(z_i = 1 \mid \mathbf{z}_{-i}, \boldsymbol{\gamma}, \boldsymbol{\mu}, \boldsymbol{\tau}_\gamma^2) &= \frac{\exp(\eta_1) P(\gamma_i \mid \mu_{z_i=1}, \tau^2_{\gamma_{z_i=1}})}{\exp(\eta_0) P(\gamma_i \mid \mu_{z_i=0}, \tau^2_{\gamma_{z_i=0}}) + \exp(\eta_1) P(\gamma_i \mid \mu_{z_i=1}, \tau^2_{\gamma_{z_i=1}})} \\[2mm]
&= \frac{1}{1 + \exp(\eta_0 - \eta_1)\frac{P(\gamma_i \mid \mu_{z_i=0}, \tau^2_{\gamma_{z_i=0}})}{P(\gamma_i \mid \mu_{z_i=1}, \tau^2_{\gamma_{z_i=1}})}} \\[2mm]
&= \frac{1}{1 + \exp(\eta_0 - \eta_1 + \log\frac{P(\gamma_i \mid \mu_{z_i=0}, \tau^2_{\gamma_{z_i=0}})}{P(\gamma_i \mid \mu_{z_i=1}, \tau^2_{\gamma_{z_i=1}})})} \\[2mm]
&= \frac{1}{1 + \exp(-(\eta_1 - \eta_0 + \log\frac{P(\gamma_i \mid \mu_{z_i=1}, \tau^2_{\gamma_{z_i=1}})}{P(\gamma_i \mid \mu_{z_i=0}, \tau^2_{\gamma_{z_i=0}})}))} \\[2mm]
&= \mathrm{sigmoid}\left(\eta_1 - \eta_0 + \log\frac{P(\gamma_i \mid \mu_{z_i=1}, \tau^2_{\gamma_{z_i=1}})}{P(\gamma_i \mid \mu_{z_i=0}, \tau^2_{\gamma_{z_i=0}})}\right).
\end{aligned}
$$

SUPPLEMENTARY MATERIAL

REFERENCES

AGUIRRE, A. J., MEYERS, R. M., WEIR, B. A., VAZQUEZ, F., ZHANG, C.-Z., BEN-DAVID, U., COOK, A., HA, G., HARRINGTON, W. F. et al. (2016). Genomic copy number dictates a gene-independent cell response to CRISPR/Cas9 targeting. *Cancer Discov.* **6** 914–929.

BALDI, P., CHAUVIN, Y., HUNKAPILLER, T. and MCCLURE, M. A. (1994). Hidden Markov models of biological primary sequence information. *Proc. Natl. Acad. Sci. USA* **91** 1059–1063.

BETANCOURT, M. (2017). A conceptual introduction to Hamiltonian Monte Carlo. Preprint. Available at arXiv:1701.02434.

BETANCOURT, M. and GIROLAMI, M. (2015). Hamiltonian Monte Carlo for hierarchical models. In *Current Trends in Bayesian Methodology with Applications* 79–101. CRC Press, Boca Raton, FL. MR3644666

CHEN, M., CHO, J. and ZHAO, H. (2011). Incorporating biological pathways via a Markov random field model in genome-wide association studies. *PLoS Genet.* **7** e1001353.

CHEN, X., SHI, X., XU, X., WANG, Z., MILLS, R., LEE, C. and XU, J. (2012). A two-graph guided multi-task lasso approach for eQTL mapping. In *International Connference on Artificial Intelligence and Statistics* 208–217.

COWLEY, G. S., WEIR, B. A., VAZQUEZ, F., TAMAYO, P., SCOTT, J. A., RUSIN, S., EAST-SELETSKY, A., ALI, L. D., GERATH, W. F. et al. (2014). Parallel genome-scale loss of function screens in 216 cancer cell lines for the identification of context-specific genetic dependencies. *Sci. Data* **1** 140035.

DE LUIS BALAGUER, M. A. and SOZZANI, R. (2017). Inferring gene regulatory networks in the arabidopsis root using a dynamic Bayesian network approach. In *Plant Gene Regulatory Networks* 331–348. Springer, New York.

DEPMAP, BROAD (2019). DepMap Achilles 19Q1 Public. Fileset on figshare. https://doi.org/10.6084/m9.figshare.7655150.v2

DIRMEIER, S. and BEERENWINKEL, N. (2022). Supplement to "Structured hierarchical models for probabilistic inference from perturbation screening data." https://doi.org/10.1214/21-AOAS1580SUPPA, https://doi.org/10.1214/21-AOAS1580SUPPB

DIRMEIER, S., FUCHS, C., MUELLER, N. S. and THEIS, F. J. (2017). netReg: Network-regularized linear models for biological association studies. *Bioinformatics* **34** 896–898.

DIRMEIER, S., DÄCHERT, C., VAN HEMERT, M., TAS, A., OGANDO, N. S., VAN KUPPEVELD, F., BARTENSCHLAGER, R., KADERALI, L., BINDER, M. et al. (2020). Host factor prioritization for pan-viral genetic perturbation screens using random intercept models and network propagation. *PLoS Comput. Biol.* **16** 1–19.

DOENCH, J. G., HARTENIAN, E., GRAHAM, D. B., TOTHOVA, Z., HEGDE, M., SMITH, I., SULLENDER, M., EBERT, B. L., XAVIER, R. J. et al. (2014). Rational design of highly active sgRNAs for CRISPR-Cas9-mediated gene inactivation. *Nat. Biotechnol.* **32** 1262–1267.

DOENCH, J. G., FUSI, N., SULLENDER, M., HEGDE, M., VAIMBERG, E. W., DONOVAN, K. F., SMITH, I., TOTHOVA, Z., WILEN, C. et al. (2016). Optimized sgRNA design to maximize activity and minimize off-target effects of CRISPR-Cas9. *Nat. Biotechnol.* **34** 184–191.

DOUDNA, J. A. and CHARPENTIER, E. (2014). Genome editing. The new frontier of genome engineering with CRISPR-Cas9. *Science* **346** 1258096. https://doi.org/10.1126/science.1258096

DURBIN, R., EDDY, S. R., KROGH, A. and MITCHISON, G. (1998). *Biological Sequence Analysis*: *Probabilistic Models of Proteins and Nucleic Acids*. Cambridge Univ. Press, Cambridge.

EDDY, S. R. (1998). Profile hidden Markov models. *Bioinformatics* **14** 755–763.

EFRON, B. (2012). *Large-Scale Inference*: *Empirical Bayes Methods for Estimation*, *Testing*, *and Prediction*. *Institute of Mathematical Statistics* (*IMS*) *Monographs* **1**. Cambridge Univ. Press, Cambridge. MR2724758 https://doi.org/10.1017/CBO9780511761362

FINN, R. D., CLEMENTS, J. and EDDY, S. R. (2011). HMMER web server: Interactive sequence similarity searching. *Nucleic Acids Res.* **39** W29–W37. https://doi.org/10.1093/nar/gkr367

FRIEDMAN, N., LINIAL, M., NACHMAN, I. and PE'ER, D. (2000). Using Bayesian networks to analyze expression data. *J. Comput. Biol.* **7** 601–620.

FUSI, N., LIPPERT, C., LAWRENCE, N. D. and STEGLE, O. (2014). Warped linear mixed models for the genetic analysis of transformed phenotypes. *Nat. Commun.* **5** 4890. https://doi.org/10.1038/ncomms5890

GABRY, J., SIMPSON, D., VEHTARI, A., BETANCOURT, M. and GELMAN, A. (2019). Visualization in Bayesian workflow. *J. Roy. Statist. Soc. Ser. A* **182** 389–402. MR3902665 https://doi.org/10.1111/rssa.12378

GELMAN, A. (2006). Prior distributions for variance parameters in hierarchical models (comment on article by Browne and Draper). *Bayesian Anal.* **1** 515–533. MR2221284 https://doi.org/10.1214/06-BA117A

GELMAN, A. and SHALIZI, C. R. (2013). Philosophy and the practice of Bayesian statistics. *Br. J. Math. Stat. Psychol.* **66** 8–38. MR3044854 https://doi.org/10.1111/j.2044-8317.2011.02037.x

GELMAN, A., SIMPSON, D. and BETANCOURT, M. (2017). The prior can often only be understood in the context of the likelihood. *Entropy* **19** 555.

GELMAN, A., CARLIN, J. B., STERN, H. S., DUNSON, D. B., VEHTARI, A. and RUBIN, D. B. (2013). *Bayesian Data Analysis*, 3rd ed. *Texts in Statistical Science Series*. CRC Press, Boca Raton, FL. MR3235677

GUO, Y. and SCHUURMANS, D. (2006). Convex structure learning for Bayesian networks: Polynomial feature selection and approximate ordering. In *Proceedings of the Twenty-Second Conference on Uncertainty in Artificial Intelligence*. UAI'06.

HAGBERG, A., SCHULT, D. and SWART, P. (2008). Exploring network structure, dynamics, and function using NetworkX. In *Proceedings of the 7th Python in Science Conference* 11–15.

HART, T., BROWN, K. R., SIRCOULOMB, F., ROTTAPEL, R. and MOFFAT, J. (2014). Measuring error rates in genomic perturbation screens: Gold standards for human functional genomics. *Mol. Syst. Biol.* **10** 733.

HART, T., CHANDRASHEKHAR, M., AREGGER, M., STEINHART, Z., BROWN, K. R., MACLEOD, G., MIS, M., ZIMMERMANN, M., FRADET-TURCOTTE, A. et al. (2015). High-resolution CRISPR screens reveal fitness genes and genotype-specific cancer liabilities. *Cell* **163** 1515–1526.

HAWE, J. S., THEIS, F. J. and HEINIG, M. (2019). Inferring interaction networks from multi-omics data. *Front. Genet.* **10** 535. https://doi.org/10.3389/fgene.2019.00535

HOFFMAN, M. D. and GELMAN, A. (2014). The no-U-turn sampler: Adaptively setting path lengths in Hamiltonian Monte Carlo. *J. Mach. Learn. Res.* **15** 1593–1623. MR3214779

IMKELLER, K., AMBROSI, G., BOUTROS, M. and HUBER, W. (2019). Modelling asymmetric count ratios in CRISPR screens to decrease experiment size and improve phenotype detection. *BioRxiv*.

JANG, E., GU, S. and POOLE, B. (2017). Categorical reparameterization with Gumbel-Softmax. In *International Conference on Learning Representations*.

JANSEN, R., YU, H., GREENBAUM, D., KLUGER, Y., KROGAN, N. J., CHUNG, S., EMILI, A., SNYDER, M., GREENBLATT, J. F. et al. (2003). A Bayesian networks approach for predicting protein-protein interactions from genomic data. *Science* **302** 449–453.

JINEK, M., CHYLINSKI, K., FONFARA, I., HAUER, M., DOUDNA, J. A. and CHARPENTIER, E. (2012). A programmable dual-RNA-guided DNA endonuclease in adaptive bacterial immunity. *Science* **337** 816–821.

KASS, R. E. and NATARAJAN, R. (2006). A default conjugate prior for variance components in generalized linear mixed models (comment on article by Browne and Draper). *Bayesian Anal.* **1** 535–542. MR2221285 https://doi.org/10.1214/06-BA117B

KASS, R. E. and WASSERMAN, L. (1996). The selection of prior distributions by formal rules. *J. Amer. Statist. Assoc.* **91** 1343–1370.

KIM, S. and XING, E. P. (2012). Tree-guided group lasso for multi-response regression with structured sparsity, with an application to EQTL mapping. *Ann. Appl. Stat.* **6** 1095–1117. MR3012522 https://doi.org/10.1214/12-AOAS549

KOLLER, D. and FRIEDMAN, N. (2009). *Probabilistic Graphical Models*: *Principles and Techniques*. *Adaptive Computation and Machine Learning*. MIT Press, Cambridge, MA. MR2778120

KORTE, A., VILHJÁLMSSON, B. J., SEGURA, V., PLATT, A., LONG, Q. and NORDBORG, M. (2012). A mixed-model approach for genome-wide association studies of correlated traits in structured populations. *Nat. Genet.* **44** 1066–1071.

KRUMSIEK, J., SUHRE, K., ILLIG, T., ADAMSKI, J. and THEIS, F. J. (2011). Gaussian graphical modeling reconstructs pathway reactions from high-throughput metabolomics data. *BMC Syst. Biol.* **5** 21. https://doi.org/10.1186/1752-0509-5-21

KUIPERS, J., THURNHERR, T., MOFFA, G., SUTER, P., BEHR, J., GOOSEN, R., CHRISTOFORI, G. and BEERENWINKEL, N. (2018). Mutational interactions define novel cancer subgroups. *Nat. Commun.* **9** 4353. https://doi.org/10.1038/s41467-018-06867-x

LI, C. and LI, H. (2008). Network-constrained regularization and variable selection for analysis of genomic data. *Bioinformatics* **24** 1175–1182.

LI, Z., LI, P., KRISHNAN, A. and LIU, J. (2011). Large-scale dynamic gene regulatory network inference combining differential equation models with local dynamic Bayesian network analysis. *Bioinformatics* **27** 2686–2691.

LI, W., XU, H., XIAO, T., CONG, L., LOVE, M. I., ZHANG, F., IRIZARRY, R. A., LIU, J. S., BROWN, M. et al. (2014). MAGeCK enables robust identification of essential genes from genome-scale CRISPR/Cas9 knockout screens. *Genome Biol.* **15** 554.

LOH, P.-R., TUCKER, G., BULIK-SULLIVAN, B. K., VILHJALMSSON, B. J., FINUCANE, H. K., SALEM, R. M., CHASMAN, D. I., RIDKER, P. M., NEALE, B. M. et al. (2015). Efficient Bayesian mixed-model analysis increases association power in large cohorts. *Nat. Genet.* **47** 284–290.

LOVE, M. I., HUBER, W. and ANDERS, S. (2014). Moderated estimation of fold change and dispersion for RNA-seq data with DESeq2. *Genome Biol.* **15** 550. https://doi.org/10.1186/s13059-014-0550-8

MAATHUIS, M., DRTON, M., LAURITZEN, S. and WAINWRIGHT, M., eds. (2018). *Handbook of Graphical Models*. *Chapman & Hall/CRC Handbooks of Modern Statistical Methods*. CRC Press, Boca Raton, FL. MR3889064

MARIONI, J. C., THORNE, N. P. and TAVARÉ, S. (2006). BioHMM: A heterogeneous hidden Markov model for segmenting array CGH data. *Bioinformatics* **22** 1144–1146.

MEYERS, R. M., BRYAN, J. G., MCFARLAND, J. M., WEIR, B. A., SIZEMORE, A. E., XU, H., DHARIA, N. V., MONTGOMERY, P. G., COWLEY, G. S. et al. (2017). Computational correction of copy number effect improves specificity of CRISPR–Cas9 essentiality screens in cancer cells. *Nat. Genet.* **49** 1779–1784.

MUNOZ, D. M., CASSIANI, P. J., LI, L., BILLY, E., KORN, J. M., JONES, M. D., GOLJI, J., RUDDY, D. A., YU, K. et al. (2016). CRISPR screens provide a comprehensive assessment of cancer vulnerabilities but generate false-positive hits for highly amplified genomic regions. *Cancer Discov.* **6** 900–913.

MURPHY, K., MIAN, S. et al. (1999). Modelling gene expression data using dynamic Bayesian networks. Technical report, Computer Science Division, Univ. California.

NEAL, R. M. (2011). MCMC using Hamiltonian dynamics. In *Handbook of Markov Chain Monte Carlo*. *Chapman & Hall/CRC Handb. Mod. Stat. Methods* 113–162. CRC Press, Boca Raton, FL. MR2858447

ONG, S. H., LI, Y., KOIKE-YUSA, H. and YUSA, K. (2017). Optimised metrics for CRISPR-KO screens with second-generation gRNA libraries. *Sci. Rep.* **7** 7384.

OUGHTRED, R., STARK, C., BREITKREUTZ, B.-J., RUST, J., BOUCHER, L., CHANG, C., KOLAS, N., O'DONNELL, L., LEUNG, G. et al. (2018). The BioGRID interaction database: 2019 update. *Nucleic Acids Res.* **47** D529–D541.

PATEL, S. J., SANJANA, N. E., KISHTON, R. J., EIDIZADEH, A., VODNALA, S. K., CAM, M., GARTNER, J. J., JIA, L., STEINBERG, S. M. et al. (2017). Identification of essential genes for cancer immunotherapy. *Nature* **548** 537–542.

RAKITSCH, B., LIPPERT, C., STEGLE, O. and BORGWARDT, K. (2012). A lasso multi-marker mixed model for association mapping with population structure correction. *Bioinformatics* **29** 206–214.

RÄMÖ, P., DREWEK, A., ARRIEUMERLOU, C., BEERENWINKEL, N., BEN-TEKAYA, H., CARDEL, B., CASANOVA, A., CONDE-ALVAREZ, R., COSSART, P. et al. (2014). Simultaneous analysis of large-scale RNAi screens for pathogen entry. *BMC Genomics* **15** 1162.

ROBINSON, M. D., MCCARTHY, D. J. and SMYTH, G. K. (2010). edgeR: A bioconductor package for differential expression analysis of digital gene expression data. *Bioinformatics* **26** 139–140.

SACHS, K., PEREZ, O., PE'ER, D., LAUFFENBURGER, D. A. and NOLAN, G. P. (2005). Causal protein-signaling networks derived from multiparameter single-cell data. *Science* **308** 523–529.

SALVATIER, J., WIECKI, T. V. and FONNESBECK, C. (2016). Probabilistic programming in Python using PyMC3. *PeerJ Comput. Sci.* **2** e55.

SCHMICH, F., SZCZUREK, E., KREIBICH, S., DILLING, S., ANDRITSCHKE, D., CASANOVA, A., LOW, S. H., EICHER, S., MUNTWILER, S. et al. (2015). gespeR: A statistical model for deconvoluting off-target-confounded RNA interference screens. *Genome Biol.* **16** 220.

SCHUBERT, B., MADDAMSETTI, R., NYMAN, J., FARHAT, M. R. and MARKS, D. S. (2019). Genome-wide discovery of epistatic loci affecting antibiotic resistance in *Neisseria gonorrhoeae* using evolutionary couplings. *Nat. Microbiol.* **4** 328–338. https://doi.org/10.1038/s41564-018-0309-1

STANKE, M. and WAACK, S. (2003). Gene prediction with a hidden Markov model and a new intron submodel. *Bioinformatics* **19** ii215–ii225.

SZKLARCZYK, D., GABLE, A. L., LYON, D., JUNGE, A., WYDER, S., HUERTA-CEPAS, J., SIMONOVIC, M., DONCHEVA, N. T., MORRIS, J. H. et al. (2018). STRING v11: Protein–protein association networks with increased coverage, supporting functional discovery in genome-wide experimental datasets. *Nucleic Acids Res.* **47** D607–D613.

TSHERNIAK, A., VAZQUEZ, F., MONTGOMERY, P. G., WEIR, B. A., KRYUKOV, G., COWLEY, G. S., GILL, S., HARRINGTON, W. F., PANTEL, S. et al. (2017). Defining a cancer dependency map. *Cell* **170** 564–576.

WAINWRIGHT, M. J. and JORDAN, M. I. (2008). Graphical models, exponential families, and variational inference. *Found. Trends Mach. Learn.* **1** 1–305.

WEI, Z. and LI, H. (2007). A Markov random field model for network-based analysis of genomic data. *Bioinformatics* **23** 1537–1544.

WEI, Z. and LI, H. (2008). A hidden spatial-temporal Markov random field model for network-based analysis of time course gene expression data. *Ann. Appl. Stat.* **2** 408–429. MR2415609 https://doi.org/10.1214/07--AOAS145

WU, G., FENG, X. and STEIN, L. (2010). A human functional protein interaction network and its application to cancer data analysis. *Genome Biol.* **11** R53. https://doi.org/10.1186/gb-2010-11-5-r53

WU, X., SCOTT, D. A., KRIZ, A. J., CHIU, A. C., HSU, P. D., DADON, D. B., CHENG, A. W., TREVINO, A. E., KONERMANN, S. et al. (2014). Genome-wide binding of the CRISPR endonuclease Cas9 in mammalian cells. *Nat. Biotechnol.* **32** 670–676.

XU, H., XIAO, T., CHEN, C.-H., LI, W., MEYER, C. A., WU, Q., WU, D., CONG, L., ZHANG, F. et al. (2015). Sequence determinants of improved CRISPR sgRNA design. *Genome Res.* **25** 1147–1157.

YOON, B.-J. (2009). Hidden Markov models and their applications in biological sequence analysis. *Curr. Genomics* **10** 402–415.

ZAMORA-RESENDIZ, R. and CRIVELLI, S. (2019). Structural learning of proteins using graph convolutional neural networks. *BioRxiv*.

ZHOU, X. and STEPHENS, M. (2012). Genome-wide efficient mixed-model analysis for association studies. *Nat. Genet.* **44** 821–824.

ZHU, S., CAO, Z., LIU, Z., HE, Y., WANG, Y., YUAN, P., LI, W., TIAN, F., BAO, Y. et al. (2019). Guide RNAs with embedded barcodes boost CRISPR-pooled screens. *Genome Biol.* **20** 20.

ZITNIK, M., AGRAWAL, M. and LESKOVEC, J. (2018). Modeling polypharmacy side effects with graph convolutional networks. *Bioinformatics* **34** i457–i466. https://doi.org/10.1093/bioinformatics/bty294

ZOU, M. and CONZEN, S. D. (2004). A new dynamic Bayesian network (DBN) approach for identifying gene regulatory networks from time course microarray data. *Bioinformatics* **21** 71–79.